

## $^{12}\text{C}(^7\text{Li}, t)^{16}\text{O}$ AND STELLAR HELIUM FUSION

F. D. BECCHETTI †

*Department of Physics, University of Michigan, Ann Arbor, Michigan 48109, USA*  
 and

*Los Alamos Scientific Laboratory, Los Alamos, New Mexico 47544, USA* ††

and

E. R. FLYNN, D. L. HANSON and J. W. SUNIER

*Los Alamos Scientific Laboratory, Los Alamos, New Mexico 47544, USA* ††

Received 8 August 1977

(Revised 13 April 1978)

**Abstract:** The reaction  $^{12}\text{C}(^7\text{Li}, t)^{16}\text{O}$  has been studied at  $E(^7\text{Li}) = 34$  MeV with the LASL tandem accelerator and QDDD magnetic spectrometer. Angular distributions to levels with  $E_x < 11$  MeV have been obtained from  $0^\circ$  to  $90^\circ$ , including  $0^\circ$ . The results have been analyzed with finite-range distorted-wave Born approximation theory. The  $\alpha$ -particle spectroscopic factors and reduced widths obtained are compared with those calculated with group theory (SU(3)) and other models. The analysis of data for the 7.1 and 9.6 MeV  $J^\pi = 1^-$  levels, which are of great importance in stellar helium burning, yields a ratio,  $R$ , of dimensionless reduced  $\alpha$ -widths  $\theta_\alpha^2(7.1 \text{ MeV})/\theta_\alpha^2(9.6 \text{ MeV}) = 0.35 \pm 0.13$ . The observed line width of the 9.6 MeV level ( $\Gamma_{\text{c.m.}} = 390 \pm 60$  keV) is less than the accepted value ( $\Gamma_{\text{c.m.}} = 510 \pm 60$  keV) and implies  $\theta_\alpha^2(9.6 \text{ MeV}) \approx 0.6$ . These results as well as data for the 6.92 MeV  $J^\pi = 2^+$  and 10.35 MeV  $J^\pi = 4^+$  “ $\alpha$ -cluster” states indicate  $0.09 < \theta_\alpha^2(7.1 \text{ MeV}) < 0.33$  with a mean value  $\theta_\alpha^2(7.1 \text{ MeV}) = 0.14 \pm 0.04$ . The implication for stellar helium burning is discussed.

E

NUCLEAR REACTIONS  $^{12}\text{C}(^7\text{Li}, t)$ ,  $E = 34$  MeV; measured  $\sigma(E, \theta)$ ,  $\Gamma_{\text{c.m.}}$ .  $^{16}\text{O}$  levels deduced  $S_\alpha$ , reduced  $\gamma_\alpha^2$ . Inferred stellar helium fusion rate. Magnetic spectrometer.

### 1. Introduction

Among all the important reaction rates required in the calculation of stellar evolution, the helium burning rate from  $^{12}\text{C}(\alpha, \gamma)^{16}\text{O}$  is at present the most uncertain<sup>1)</sup>. Knowledge of this rate is crucial in determining the mass fraction of carbon relative to oxygen in stars at the end of the helium burning phase<sup>2–4)</sup>. The course of further stellar evolution, in turn, depends on the C/O mass fraction.

† Supported in part by the National Science Foundation.

†† Supported by US Department of Energy.

The cross section for  $^{12}\text{C}(\alpha, \gamma)^{16}\text{O}$  at stellar temperatures ( $E_\alpha \approx 300$  keV) is largely determined by two  $J^\pi = 1^-$  levels in  $^{16}\text{O}$  (see fig. 1). The dominant state is the broad  $1^-$  level at  $E_x = 9.6$  MeV ( $\Gamma_\alpha \approx 0.5$  MeV). A second  $1^-$  level ( $E_x = 7.12$  MeV) although bound by 43 keV to  $\alpha$ -decay can nonetheless interfere and distort the tail of the unbound 9.6 MeV level near the  $^{12}\text{C} + \alpha$  threshold. One can show that the  $^{12}\text{C}(\alpha, \gamma)^{16}\text{O}$  cross section at  $E \lesssim 300$  keV depends on the  $\alpha$ -widths,  $\gamma_\alpha^2$ , of both the 7.12 and 9.6 MeV  $J^\pi = 1^-$  levels<sup>1-3</sup>). The  $\alpha$ -widths of the  $J^\pi = 2^+$  levels at  $E_x = 6.92$  and 9.85 MeV also may be relevant, but are not thought to be as important<sup>1</sup>).

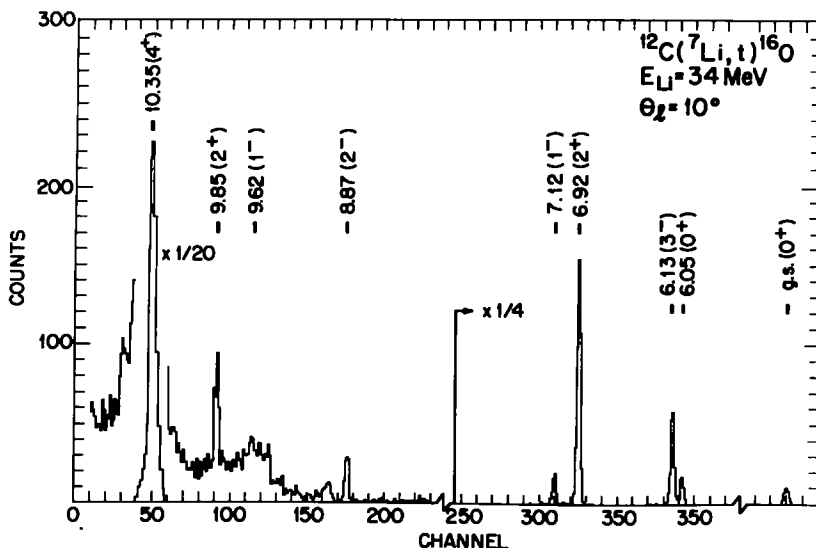


Fig. 1. A triton spectrum obtained at  $10^\circ$  (lab). The spin, parity and excitation energy (MeV) of known levels in  $^{16}\text{O}$  are indicated. The ground-state peak has been shifted to the left from its actual position.

Attempts to measure directly the  $^{12}\text{C}(\alpha, \gamma)^{16}\text{O}$  cross section at energies of astrophysical interest are hampered by the extremely small cross sections ( $\sigma < 10^{-3}$  nb). Despite experimental difficulties,  $^{12}\text{C}(\alpha, \gamma)$  cross sections have recently been measured down to  $E_\alpha \approx 1.5$  MeV, which was sufficient to indicate the influence of the 7.12 MeV level<sup>1</sup>). Extrapolations to  $E_\alpha \approx 300$  keV have been subsequently obtained by fitting  $^{12}\text{C}(\alpha, \gamma)$  and  $^{12}\text{C}(\alpha, \alpha)$  data with  $\gamma_\alpha^2(7.1)$  and  $\gamma_\alpha^2(9.6)$  treated as a free parameters but constrained initially such that  $\gamma_\alpha^2(7.1) \ll \gamma_\alpha^2(9.6)$ .

Ideally,  $\alpha$ -widths may be measured with  $\alpha$ -transfer reactions such as ( $^6\text{Li}, d$ ), ( $^7\text{Li}, t$ ), etc. provided these are "direct"  $\alpha$ -transfers and do not proceed via a compound nucleus or a two-step mechanism. Realizing this, Loebenstein *et al.*<sup>5</sup>) measured  $^6\text{Li}(^{12}\text{C}, d)^{16}\text{O}$  at  $E(^{12}\text{C}) = 18\text{--}24$  MeV and deduced a rather small  $\gamma_\alpha^2(7.1)$  relative to  $\gamma_\alpha^2(9.6)$ . Their analysis, however, is probably not reliable since at low bombarding

energies the reaction proceeds primarily via compound nucleus formation. Similarly, other measurements of  $^{12}\text{C}(^6\text{Li}, \text{d})^{16}\text{O}$  and  $^{12}\text{C}(^7\text{Li}, \text{t})^{16}\text{O}$  at low bombarding energies ( $E < 30$  MeV) contain large non-direct reaction components<sup>6-9</sup>). The  $^{12}\text{C}(^7\text{Li}, \text{t})^{16}\text{O}$  reaction appears to be favorable in this respect<sup>8,10</sup>). Recent measurements<sup>10</sup>) at  $E(^7\text{Li}) = 38$  indicate the predominately direct nature of the ( $^7\text{Li}, \text{t}$ ) reaction at high bombarding energies. Unfortunately, these measurements did not include much forward-angle data for the 7.1 MeV level nor extensive data for the 9.6 MeV or other levels. Calculations indicate that the extrapolation of the  $^{12}\text{C}(\alpha, \gamma)^{16}\text{O}$  burning rate is determined by the  $\alpha$ -widths,  $\gamma_\alpha^2(7.1)$  and  $\gamma_\alpha^2(9.6)$ , and not necessarily the "spectroscopic factor",  $S_\alpha$  or  $\theta_\alpha^2$  of the 7.12 MeV level alone. The latter is very model dependent and cannot be easily compared between different experiments. Thus the fact that some measurements<sup>8,10</sup>) indicate  $\theta_\alpha^2(7.1) \ll 1$  does not necessarily imply  $\gamma_\alpha^2(7.1) \ll \gamma_\alpha^2(9.6)$  unless one determines  $\theta_\alpha^2(9.6)$  in the same experiment. Indeed, recent data<sup>11</sup>) for  $^{12}\text{C}(^6\text{Li}, \text{d})^{16}\text{O}$  at  $E(^6\text{Li}) = 42$  MeV indicate  $R \approx 0.6$ . Similarly, a close inspection of previous ( $^7\text{Li}, \text{t}$ ) data<sup>8,10</sup>) suggests that direct  $\alpha$ -transfer to the 7.12 and 9.6 MeV levels may be comparable, implying  $\gamma_\alpha^2(7.1) \approx \gamma_\alpha^2(9.6)$ , hence  $R \approx 1$ .

To help resolve these questions, we have studied  $^{12}\text{C}(^7\text{Li}, \text{t})^{16}\text{O}$  at  $E(^7\text{Li}) = 34$  MeV with a magnetic spectrometer. The latter permitted clean separation of the levels of interest and allowed measurements at forward angles including zero degrees. In addition to the  $1^-$  levels of astrophysical interest, data for the other low-lying states afford comparison with recent calculations of  $\alpha$ -spectroscopic factors using SU(3) wave functions<sup>12</sup>) and the orthogonality condition model (OCM)<sup>13</sup>).

## 2. Experimental method

The experiment was done at the LASL tandem laboratory with a 34.0 MeV  $^7\text{Li}^{3+}$  beam. Natural carbon foils (98.9%  $^{12}\text{C}$ ), 40  $\mu\text{g}/\text{cm}^2$  and 175  $\mu\text{g}/\text{cm}^2$  thick, served as targets. Reaction products were momentum analyzed in a QDDD magnetic spectrometer ( $\Delta\Omega = 9.6$  msr,  $\Delta\theta = 4^\circ$  full width) and identified with a helical delay-line proportional counter<sup>15</sup>). The energy resolution was 25 to 60 keV, depending on the target and scattering angle. This was sufficient to resolve all states of interest at most scattering angles and allow measurement of line widths,  $\Gamma_{\text{c.m.}}$ , for levels with  $\Gamma_{\text{c.m.}} \gtrsim 20$  keV.

Angular distributions were obtained for the levels in  $^{16}\text{O}$ ,  $E_x < 11$  MeV. Measurements at  $\theta_{\text{lab}} = 0^\circ$  were accomplished by stopping the direct beam in a thin tantalum absorber placed at the entrance to the spectrometer. The absorber allowed tritons to pass through although degrading them in energy. The beam and target thickness were continuously monitored with a solid-state detector positioned at a forward scattering angle.

### 3. Data

#### 3.1. SPECTRA

A triton spectrum obtained at  $\theta_{\text{lab}} = 10^\circ$  is displayed in fig. 1. The spectrum shown is a composite of three spectra (denoted by break marks) normalized to the same integrated beam charge. The excitation energies and the spin and parity assignments are from a recent compilation <sup>14)</sup> except for  $E_x = 9.62$  MeV, which was determined in the present experiment. Peaks not explicitly labelled are attributed to the 1% <sup>13</sup>C in the target or other heavy impurities. Not shown in fig. 1 are data for the unresolved  $4^+ + 3^+$  doublet at  $E_x = 11.1$  MeV [ref. <sup>14)</sup>]. Transfer to the latter was observed at  $\theta_{\text{lab}} = 15^\circ$  and found to be only 15% of that for the 10.4 MeV  $4^+$  level. The selective population of the known  $\alpha$ -cluster states,  $2^+$  (6.92 MeV) and  $4^+$  (10.35 MeV), and particularly the ratio of transfer strength to the  $4^+$  levels at 10.35 and 11.1 MeV, indicates that the data are consistent with a direct  $\alpha$ -transfer mechanism, at least at forward angles. An indication of the non-direct transfer strength is the cross section to the  $2^-$  unnatural parity state at  $E_x = 8.87$  MeV as this state cannot be formed as the result of a simple, direct  $\alpha$ -transfer. The cross section

TABLE I  
Levels in <sup>16</sup>O

$E_x^a)$ (MeV)	$J^\pi^a)$	$\Gamma_{\text{c.m.}}$ (keV)		$\sigma_{\text{exp}}^c)$ (b)	$\sigma_{\text{HF}}^d)$ (b)	$\sigma_{\text{dir}}^e)$ (b)
		this work <sup>b)</sup>	accepted value <sup>a)</sup>			
g.s.	$0^+$			51	13 <sup>f)</sup>	38
6.049	$0^+$			64	13	51
6.130	$3^-$			385	89	296
6.917	$2^+$			808	89	719
7.117	$1^-$			95	41	54
8.872	$2^-$	< 20		53	53 <sup>g)</sup>	0 <sup>h)</sup>
9.62 ± 0.02 <sup>b)</sup>	$1^-$	390 ± 60	510 ± 60	178	28	150
9.847	$2^+$	< 20	0.9 ± 0.3	72	62	10
10.353	$4^+$	35 ± 5	27 ± 4	3468	125	3343
10.952	$0^-$					
11.080	$3^+$		< 12			
11.095	$4^+$	{ < 30	0.28 ± 0.05	{ 480 <sup>i)</sup>	230	250 <sup>j)</sup>

<sup>a)</sup> Unless otherwise noted the quantities listed have been taken from the compilation of ref. <sup>14)</sup>. The errors quoted for  $E_x$  are generally less than ±5 keV.

<sup>b)</sup> The quantity listed is the observed line width (FWHM). The accepted " $\Gamma_{\text{c.m.}}$ " include both line widths and resonance widths, which may differ (see text).

<sup>c)</sup> Experimental cross sections integrated from  $\theta_{\text{c.m.}} = 0^\circ$  to  $90^\circ$ . Estimated errors: ±15% absolute; ±5% relative.

<sup>d)</sup> Calculated Hauser-Feshbach cross sections integrated from  $\theta_{\text{c.m.}} = 0^\circ$  to  $90^\circ$ .

<sup>e)</sup> Net integrated "direct" transfer cross section  $\equiv \sigma_{\text{exp}} - \sigma_{\text{HF}}$ .

<sup>f)</sup> Reduced by  $\frac{1}{3}$  relative to the other HF calculations (see text).

<sup>g)</sup> HF calculations normalized such that  $\sigma_{\text{dir}} = 0$  for the 8.87 MeV  $2^-$  level.

<sup>h)</sup> Measured in this work [the value adopted in ref. <sup>14)</sup> is  $9.632 \pm 0.021$  MeV].

<sup>i)</sup> Estimated from forward angle cross sections and therefore uncertain by a factor of two or more.

to this state is seen to be about 10% of the 6.92 MeV  $2^+$  “ $\alpha$ -cluster” state yet comparable to that of the non- $\alpha$ -cluster 9.85 MeV  $2^+$  level<sup>12</sup>). The 9.6 MeV  $1^-$  level is observed to be only a factor of two or so stronger than the 7.12 MeV  $1^-$  level, while both are substantially more intense, after including  $2J+1$  statistical factors, than the transitions to the 8.87 MeV  $2^-$  and 9.85 MeV  $2^+$  levels. In addition, a comparison of cross sections to the 7.12 MeV  $1^-$  level and the  $2^+$  “ $\alpha$ -cluster” state at 6.92 MeV, again scaling for  $2J+1$  statistical factors, also suggests that the former has an appreciable non-compound component. These conclusions are consistent with the theoretical analysis (sect. 4).

The energy resolution obtained (fig. 1) permits direct measurement of the line width,  $\Gamma_{\text{c.m.}}$ , of the  $\alpha$ -unbound levels  $E_x > 7.2$  MeV, particularly the 9.6 MeV  $1^-$  level. In addition, the centroid of the  $1^-$  level was determined using the known excitation energies<sup>14</sup>) of nearby levels. The widths and excitation energies are listed in table 1.

Data obtained in the region of the  $4^+$  (10.35 MeV),  $2^+$  (9.85 MeV) and  $1^-$  (9.6 MeV) levels are shown in fig. 2. Also shown are curves fitted to the data in a least-squares fashion utilizing a combination of Gaussian and Lorentzian line shapes. The particular fits shown indicate  $\Gamma_{\text{c.m.}}(9.6 \text{ MeV}) \approx 350$  keV. Other, equally acceptable fits

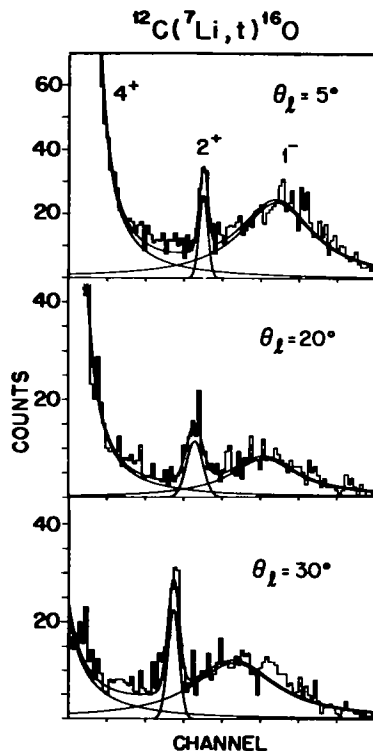


Fig. 2. Spectra near  $E_x = 9.6$  MeV. The curves shown are three-level fits to the data (see text).

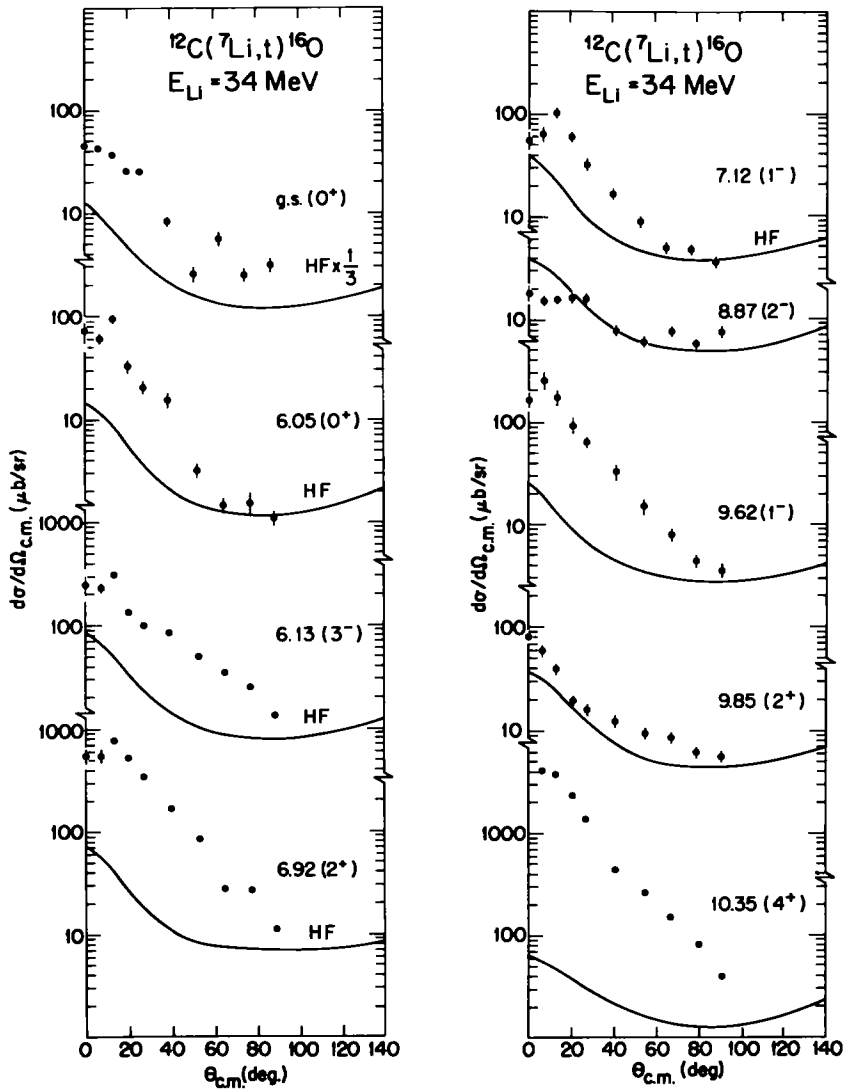


Fig. 3. Experimental angular distributions. The solid curves are Hauser-Feshbach calculations normalized to the  $2^-$  level at 8.87 MeV, except for the g.s. which has been reduced an additional factor of  $\frac{1}{3}$ .

( $\chi^2/N \approx 1$ ) could be obtained with  $\Gamma_{c.m.} = 300$  to 450 keV depending on the contributions allowed from broad levels at high excitations, etc. The mean value and standard deviation is  $\Gamma_{c.m.}(9.6 \text{ MeV}) = 390 \pm 60 \text{ keV}$ .

The line width observed for the 9.6 MeV level is smaller than the accepted value <sup>14)</sup> by about 100 keV but is not necessarily the intrinsic decay width  $\Gamma_a$  as we are observing an outgoing triton. Any energy dependence of the ( ${}^7\text{Li}, t$ ) cross section or perturbation

caused by the  $^7\text{Li}$  or triton projectiles could distort the line shape although calculations indicate these have only a slight effect ( $< 10$  keV). A smaller  $\Gamma_\alpha$ , of course, affects the value of  $S_\alpha$  (or  $\gamma_\alpha^2$ ) deduced for this state from the line width (see subsect. 4.3). The line width observed in  $(^7\text{Li}, t)$  is comparable to that observed  $^{11}$ ) in  $^{12}\text{C}(^6\text{Li}, d)$ , viz.  $\Gamma_{\text{c.m.}} = 400 \pm 50$  keV.

### 3.2. CROSS SECTIONS

Differential cross sections are displayed in fig. 3. Also shown are Hauser-Feshbach (HF) calculations for non-direct statistical compound nuclear cross sections  $^{10}$ ). The HF curves have been re-normalized by a common factor determined by fitting data for the  $2^-$  level. In addition, the HF calculation for the  $0^+$  g.s. has been further reduced ( $\times \frac{1}{3}$ ) so as not to overestimate the cross sections at large angles. A similar problem has been observed for  $^{12}\text{C}(^6\text{Li}, d)^{16}\text{O}(\text{g.s.})$  [ref.  $^{11}$ ].

The HF calculations, in general, account for most of the cross sections beyond  $\theta_{\text{lab}} \approx 70^\circ$  and, if anything, overestimate the non-direct component for  $J^\pi < 2$  and/or  $E_x < 8.8$  MeV, as seen explicitly for the  $0^+$  g.s. The cross sections for all but the  $2^-$  (8.87 MeV) and  $2^+$  (9.85 MeV) states exhibit a substantial forward peaking, although without notable structure except perhaps for the  $0^+$  g.s. The forward rise of the cross sections appear to be correlated with  $J$ , with  $J = 4$  the most steep followed by  $J = 3$  and 2 and then  $J = 1$  and 0. The shape of the angular distributions for the 9.6 and 7.12 MeV  $1^-$  levels are essentially identical to within experimental uncertainties. The errors shown for the 9.6 MeV state are due primarily to uncertainties in the exact line shape for this state and to the contribution of the other nearby levels ( $2^+$  9.85 MeV and  $4^+$  10.35 MeV). The various peak-fitting methods employed gave results consistent to  $\pm 15\%$ . Particular care was taken to include realistic "tails" for the 9.6 MeV level so as to not underestimate the cross section.

Integrated cross sections,  $\sigma_{\text{exp}}$ , are listed in table 1, together with the corresponding calculated HF cross section,  $\sigma_{\text{HF}}$ . We will denote the quantity  $\sigma_{\text{dir}} \equiv \sigma_{\text{exp}} - \sigma_{\text{HF}}$  as the net "direct" component. We observe  $\sigma_{\text{exp}}(7.1)/\sigma_{\text{exp}}(9.6) \approx 0.53$  with  $\sigma_{\text{dir}}(7.1)/\sigma_{\text{dir}}(9.6) \approx 0.36$ . The latter is probably a lower limit as the HF calculation may be an overestimate for the 7.12 MeV state, as explained previously.

The separation of  $\sigma_{\text{dir}}$  into  $\sigma_{\text{exp}}$  and  $\sigma_{\text{HF}}$  assumes that the compound and direct mechanisms add incoherently although in theory there can be coherent interference. Except for the  $0^+$  g.s., which is likely a special case as it differs greatly in  $Q$ -value and spin from the other levels, the data are consistent with the assumption of incoherence: the large-angle data scale as expected for a compound mechanism while the forward angle data for " $\alpha$ -cluster" levels rise rapidly with decreasing angle with slopes characteristic of a direct  $\alpha$ -transfer mechanism. Also, the HF calculations indicate that  $\sigma_{\text{HF}}$  is a small ( $< 30\%$ ) contribution to the forward-angle cross sections for these levels. We therefore proceed with the proviso that our results depend on the assumption of incoherent addition of  $\sigma_{\text{HF}}$  and  $\sigma_{\text{dir}}$ , at least when  $\sigma_{\text{HF}} \ll \sigma_{\text{exp}}$ .

## 4. Analysis

### 4.1. DISTORTED-WAVE CALCULATIONS

Finite-range distorted-wave Born approximation calculations<sup>16,17</sup>, including recoil, have been performed. We define phenomenological  $\alpha$ -spectroscopic factors in analogy with single-nucleon stripping to a final state of spin  $J$  as

$$\left(\frac{d\sigma}{d\Omega}\right)^{\text{exp}} = (2J+1)S_1S_2 \sum_l C_l \left(\frac{d\sigma}{d\Omega}\right)_l^{\text{DW}}, \quad (1)$$

where  $S_1$  is the square of the overlap of the projectile ( ${}^7\text{Li}$ ) into  $\alpha+t$  and  $S_2 (= S_\alpha)$  is that of the residual nucleus ( ${}^{16}\text{O}$ ) into  $\alpha+{}^{12}\text{C}$ . The quantity  $C_l$  is an angular momentum coupling coefficient and  $(d\sigma^{\text{DW}}/d\Omega)_l$  is the distorted-wave calculation for a specific  $l$ -transfer, calculated here in the post representation with a finite-range program<sup>16</sup>). There are two  $l$ -transfers normally allowed by the angular momentum and parity selection rules,  $l = J+1$  and  $l = J-1$ . An additional, "parity-forbidden"  $l$ -transfer ( $l = J$ ) is introduced by recoil effects and is known to be critically important in heavy-ion reactions. This is found to be also true for the present analysis of ( ${}^7\text{Li}$ , t) although this  $l$ -transfer is often neglected.

The optical model potentials for the triton distorted waves were adapted from ref. 18). Several  ${}^7\text{Li}$  optical model potentials were investigated with those given by Schumacher *et al.* (set III)<sup>19</sup>) deemed as giving the best fit to the data without *ad hoc* parameter adjustments. Other  ${}^7\text{Li}$  potential sets, notably those having surface absorption<sup>10,20</sup>), yielded less satisfactory fits to the data. We compare in fig. 4 the distorted-wave plus HF calculations employing  ${}^7\text{Li}$  volume absorption<sup>19</sup>) and  ${}^7\text{Li}$  surface absorption<sup>10</sup>) with cross section data for the  $0^+$ (g.s.),  $0^+$ (6 MeV) and  $1^-(7\text{ MeV})$  levels. The  $0^+$  levels are the most sensitive to optical model parameters as only small  $l$ -transfers are involved. The surface absorption calculations tend to fall off much too slowly with angle compared with the data. In particular, the important region from  $\theta = 20^\circ$  to  $50^\circ$ , which contains most of the integrated cross section, is much better reproduced utilizing volume absorption. Improved fits could be obtained with surface-absorption potentials by introducing radial cut-offs in the form factor so as to exclude contributions from the nuclear interior. The spectroscopic factors then approach those obtained with volume absorption. Similar effects have been noted in the analysis<sup>11</sup>) of  ${}^{12}\text{C}({}^6\text{Li}, d){}^{16}\text{O}$ . Finally, one observes that the relative spectroscopic factors deduced from  ${}^{12}\text{C}({}^7\text{Li}, t)$  and  ${}^{12}\text{C}({}^6\text{Li}, d)$  are at least qualitatively similar for a given level in  ${}^{16}\text{O}$  if one employs volume absorption for both  ${}^6\text{Li}$  and  ${}^7\text{Li}$ . Surface absorption potentials produce extremely non-compatible results, however. We thus adopt  ${}^7\text{Li}$  volume-absorption potentials as those most compatible with the widest range of data: elastic, inelastic and transfer reactions.

The  $\alpha+t$  cluster wave function suggested by Kubo and Hirata was used for the  ${}^7\text{Li}$  projectile ( $N, L = 1, 1$ ) [ref. 17)]. The  $\alpha$ -particle in  ${}^{16}\text{O}$  was calculated as a simple four-nucleon cluster bound in a Woods-Saxon potential with the potential depth



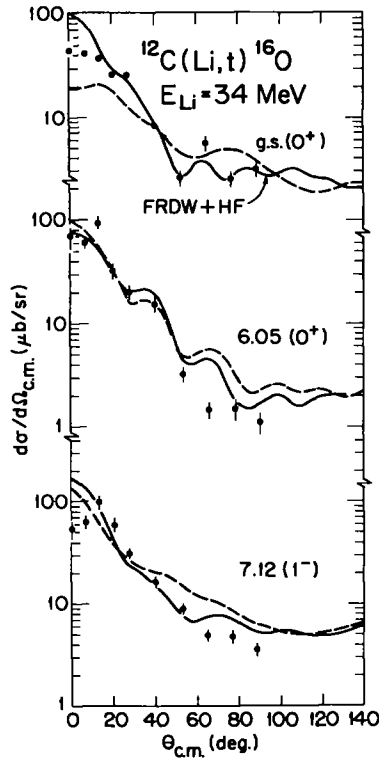


Fig. 4. Distorted-wave (FRDW) plus Hauser-Feshbach (HF) calculations. The FRDW calculations shown employ  $^7\text{Li}$  optical model potentials having either volume absorption [ref. <sup>19</sup>], solid curves] or surface absorption [ref. <sup>10</sup>], broken curves].

adjusted to fit the known  $\alpha$ -separation energy. The calculations for unbound levels ( $E_x > 7.2$  MeV) employed form factors obtained with the  $\alpha$ -cluster bound at 0.2 MeV. This should be suitable for high-spin levels ( $l > 2$ ) as the real cluster is "quasi-bound" owing to the large centrifugal barrier. The broad  $1^-$  level at 9.6 MeV was treated as follows: Calculations were performed at several  $\alpha$ -binding energies approaching zero and the resulting cross section extrapolated to the actual  $\alpha$ -separation energy. The validity of this procedure has been checked by a comparison with zero-range DWBA calculations utilizing unbound form factors <sup>21</sup>). Although some uncertainty in the spectroscopic factor is introduced ( $\pm 20\%$ ), this procedure should not have a large effect on extrapolation of the reduced width,  $\gamma_\alpha^2$ .

The quantum numbers ( $N, L$ ) for the  $\alpha$ -cluster in  $^{16}\text{O}$  were determined by the expected dominant SU(3) components of the  $^{16}\text{O}$  wave function. Extended shell-model calculations <sup>13</sup>) for  $^{16}\text{O}$  yield  $\alpha$ -cluster wave functions often having one fewer radial node,  $N$ , for certain levels compared to SU(3) or a simple shell model. We

TABLE 2  
Alpha spectroscopic factors and widths for  $^{16}\text{O}$

$J^\pi$	$E_\alpha$ (MeV)	$(\lambda\mu)^a$	$N, L^b$	$S_\alpha^c$	$S_2/S_\alpha(4^+)$	$\gamma_\alpha^2$ (5.4 fm) <sup>d</sup> (keV)	$\theta_\alpha^2$ (5.4 fm) ° <sup>e</sup>	$\theta_\alpha^2/\theta_\alpha^2(4^+)$
$0^+$	g.s.	(00)	2, 0	0.38 (0.10–0.40)	1.26 (0.41–1.0)	20	0.03	0.27 (0.03–0.34)
			(4, 0)	0.06	0.21	15	0.02	0.19
$0^+$	6.0	(84)	4, 0	0.11 (0.09–0.16)	0.35 (0.37–0.40)	49	0.07	0.63 (0.65–0.73)
			(3, 0) <sup>f</sup>	0.13	0.44	44	0.06	0.57
$3^-$	6.1	(21)	1, 3	0.09 (0.03–0.12)	0.28 (0.13–0.30)	10	0.015	0.13 (0.06–0.14)
$2^+$	6.9	(84)	3, 2	0.17 (0.13–0.23)	0.55 (0.54–0.58)	70	0.10	0.92 (0.92–0.96)
			(2, 2) <sup>f</sup>	0.17	0.58	49	0.07	0.63
$1^-$	7.1	(21)	2, 1	0.08 (0.02–0.12)	0.26 (0.08–0.30)	22	0.03	0.28 (0.09–0.32)
			(4, 1)	0.03	0.10	15	0.02	0.19
$1^-$	9.6	(94)	4, 1	0.17 (0.14–0.23) <sup>g</sup>	0.58 (0.58–0.58) <sup>g</sup>	54	0.08	0.70 (0.59–0.70)
			(3, 1) <sup>f</sup>	0.16 <sup>g</sup>	0.54 <sup>g</sup>	40	0.06	0.51
			2, 2	$\lesssim 0.002^h$	$\lesssim 0.008$	$\lesssim 0.7$	$\lesssim 0.001$	$\lesssim 0.009$
$2^+$	9.8	(84)	2, 4	0.30 (0.24–0.40)	1.0 (1.0)	78	0.11	1.0 (1.0)
$4^+$	10.3	(84)	2, 4	$\lesssim 0.02^h$	$\lesssim 0.06$	$\lesssim 5$	$\lesssim 0.007$	$\lesssim 0.06$
$4^+$	11.1		2, 4	$\lesssim 0.02^h$	$\lesssim 0.06$	$\lesssim 5$	$\lesssim 0.007$	$\lesssim 0.06$

<sup>a</sup>)  $(\lambda\mu)$  are the SU(3) quantum numbers of the theoretical model wave functions describing levels in  $^{16}\text{O}$  [ref. <sup>12</sup>].

<sup>b</sup>) The quantities  $N$  and  $L$  are the radial nodes and orbital angular momentum assigned to the c.m. motion of the  $\alpha$ -cluster in  $^{16}\text{O}$ . The corresponding FRDW form factors were generated in a Woods-Saxon potential well with  $R = 3.0$  fm,  $a = 0.73$  fm,  $R_c = 5.0$  fm, and  $V$  adjusted to fit the  $\alpha$ -separation energy for  $\alpha$ -bound levels, or a binding energy of 0.2 MeV for the unbound levels (see text). The first set of  $N$ - and  $L$ -values listed correspond to the dominant SU(3) components <sup>12</sup>). Other values used to determine  $S_\alpha$  etc. are shown in parenthesis.

<sup>c</sup>) Alpha spectroscopic factors  $S_\alpha$  ( $= S_2$ , eq. (1)) deduced from the experimental integrated cross sections and the corresponding integrated FRDW calculations using the form factor indicated. The  $^7\text{Li}$  wave function is that given in ref. <sup>17</sup>) ( $S_1 = 1$ ). The first  $S_\alpha$  values listed correspond to the  $^7\text{Li}$  optical model potentials of ref. <sup>19</sup>) (set III) while those given in parenthesis were obtained using other  $^7\text{Li}$  parameters <sup>10, 20</sup>). The triton optical model potentials are set II from ref. <sup>18</sup>). The quantity  $S_2/S_\alpha(4^+)$  is  $S_2$  relative to the  $4^+$  level at 10.3 MeV.

<sup>d</sup>) Reduced  $\alpha$ -width calculated at a channel radius of 5.4 fm inferred from the FRDW calculations (5). See text regarding absolute normalization.

<sup>e</sup>) The reduced  $\alpha$ -width divided by the Wigner limit (710 keV; eq. (6)). The quantity  $\theta_\alpha^2/\theta_\alpha^2(4^+)$  corresponds to  $\theta_\alpha^2$  relative to that for the  $4^+$  level at 10.3 MeV.

<sup>f</sup>) The values of  $N$  and  $L$  listed are those suggested by OCM calculations <sup>13</sup>).

<sup>g</sup>)  $S_\alpha$  has been increased by 40 % relative to a bound level as suggested by extrapolation of the FRDW cross sections to the correct  $\alpha$ -separation energy ( $Q_\alpha = 2.5$  MeV).

<sup>h</sup>) The values quoted are highly uncertain (factor of 2 or more) as the direct cross sections are not accurately determined (table 1).

therefore included in our analysis calculations with  $\alpha$ -cluster wave functions having different radial nodes than those suggested by SU(3) configurations.

The parameters employed in the distorted-wave calculations and the results are summarized in table 2. Fits to the data, including HF calculations, are shown in fig. 5. The overall agreement with experiment is satisfactory for most levels considering that no parameters have been adjusted. As noted previously three  $l$ -transfers con-

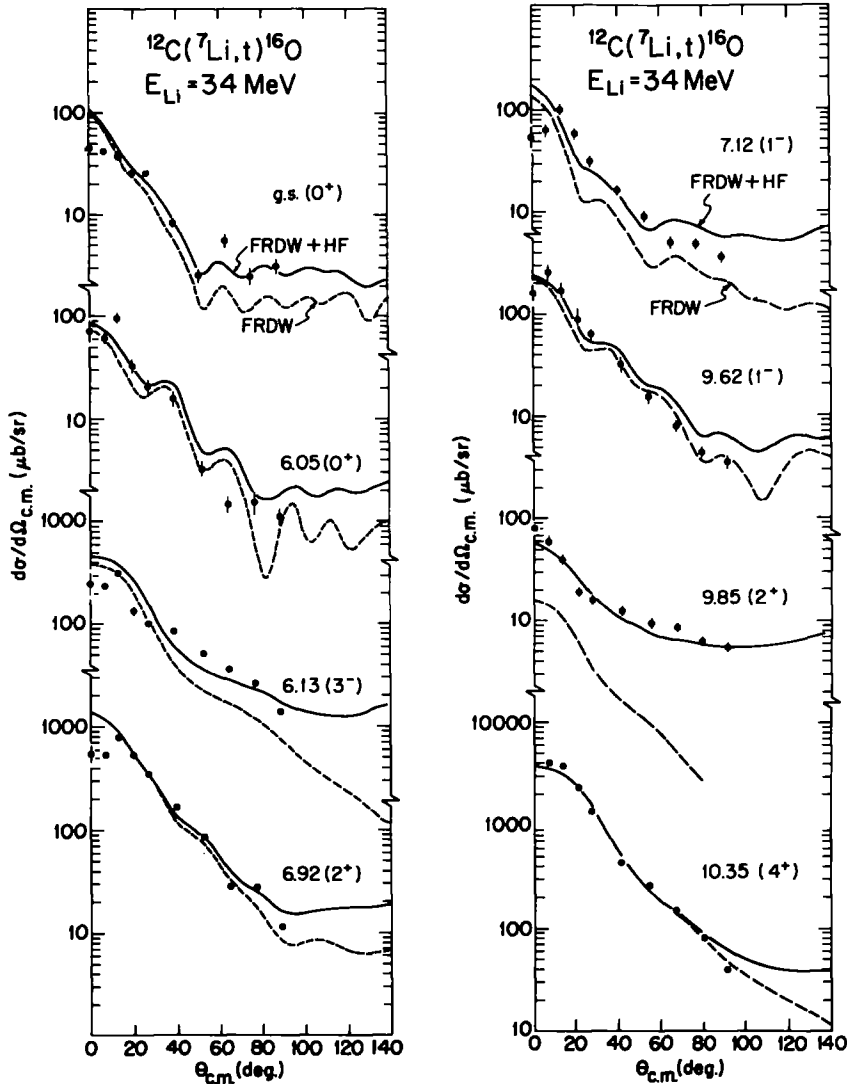


Fig. 5. Experimental angular distributions compared with finite-range distorted-wave calculations (FRDW) and the sum of the latter and the HF calculations.

tribute. The combined effect of the multiple  $l$ -transfers, particularly the recoil  $l$ -transfer, is to wash out most of the structure in the calculated angular distributions in agreement with experiment. The range of  $S_\alpha$  values obtained using different optical model parameters, etc., are given in parenthesis in table 2. The corresponding relative  $S_\alpha$  values and  $\alpha$ -widths ( $\gamma_\alpha^2$  and  $\theta_\alpha^2$ ) will have a similar range of values. Note, however, that the  $S_\alpha$  values etc. for different levels will tend to scale up and down

together for a particular parameter set so one should only compare a given set of values, not the extrema among all sets. The variations in the  $S_\alpha$  relative to our adopted values are on the order  $\pm 30\%$ . Decreasing the number of radial nodes for the  $0^+(6 \text{ MeV})$ ,  $2^+(7 \text{ MeV})$  and  $1^-(9.6 \text{ MeV})$  levels as suggested by the OCM calculations <sup>13)</sup> has a 20% to 30% effect on the values of  $S_\alpha$  and  $\gamma_\alpha^2$  deduced for these levels (see table 2).

The  $\alpha$ -spectroscopic factors obtained from our analysis (table 2) are compared in fig. 6 with those calculated from SU(3) group theory <sup>12)</sup> and the orthogonality condition model <sup>13)</sup>. In principle the  $S_\alpha$  values are "absolute" since we use a "realistic" <sup>7</sup>Li wave function and  $\alpha$ -t interaction so that the appropriate normalization is included explicitly <sup>16,17)</sup>. Although it is reassuring that the calculations and experiment are comparable in absolute value, this agreement should not be taken too seriously as there are many parameters that affect the overall magnitude of the calculated cross sections. We therefore also compare in fig. 6 experiment and calculations relative to the  $J^\pi = 4^+$  " $\alpha$ -cluster" level at 10.35 MeV.

One observes the following features: The " $\alpha$ -cluster" states ( $0^+$ , 6.05 MeV;  $2^+$ , 6.92 MeV;  $1^-$ , 9.6 MeV) have a measured  $S_\alpha$  much smaller than the calculated values,

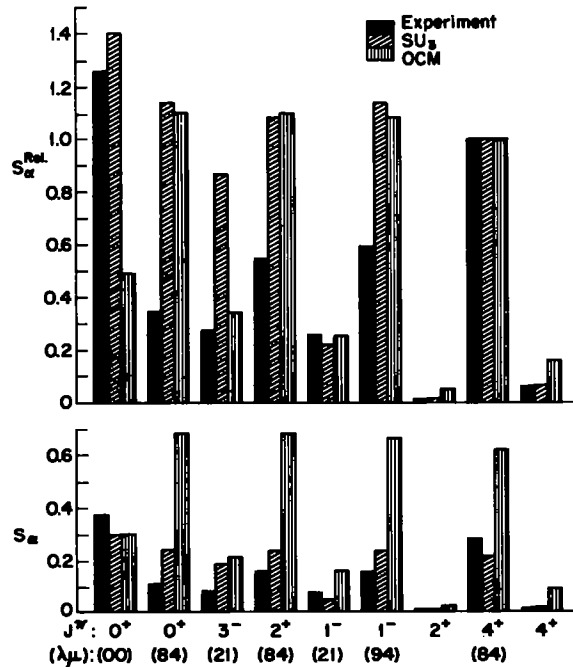


Fig. 6. Bottom: "Absolute"  $\alpha$  spectroscopic factors for levels in <sup>16</sup>O obtained in the present experiment (table 2) compared with values calculated from SU(3) and OCM theory <sup>12,13)</sup>. The leading SU(3) components are indicated by the ( $\lambda\mu$ ) indices. Top: A comparison of  $\alpha$  spectroscopic factors relative to the 10.35 MeV  $4^+$  level, where  $S_\alpha$  for the latter has been set to unity.

or at least relative to the  $4^+$  level at 10.35 MeV. The OCM correctly predicts the relative strength to the 6.13 MeV  $3^-$  and 7.12 MeV  $1^-$  levels while both SU(3) and OCM predict a small  $S_\alpha$  for the 9.85 MeV  $2^+$  and 11.1 MeV  $4^+$  states, in agreement with experiment. The  $S_\alpha$  observed for the g.s. is larger than predicted by the OCM calculation and appears to be more consistent with the simple SU(3) limit. Small admixtures of higher configurations in the g.s. form factor e.g.,  $N, L = 4, 0$  would reduce  $S_\alpha$ , however (see table 2). The  $({}^7\text{Li}, t)$  results for the 9.85 MeV  $2^+$  and 11.1 MeV  $4^+$  level are consistent with  $^{12}\text{C}(\alpha, \alpha)$  experiments and the small  $\Gamma_{\text{c.m.}}$  observed for these states (table 1). This indicates that non-direct transfer mechanisms, other than compound nucleus decay, are likely not significant, at least for these levels. The fact that  $S_\alpha < 1$  for the 7.1 MeV level is not surprising as this level is thought to be mainly a 1p-1h state. The fact that the observed  $S_\alpha$  for the 9.6 MeV  $1^-$  is substantially less than unity is unexpected as this is a member of a 4p-4h rotational band. This  $S_\alpha$  implies a ratio of  $\gamma_\alpha^2(7.1)/\gamma_\alpha^2(9.6)$  which is larger than expected. As noted above, however, other members of the 4p-4h bands also indicate  $S_\alpha$  smaller than expected. As is well known,  $\alpha$ -spectroscopic factors are model-dependent quantities (table 2) and useful primarily in testing specific calculations. The more model-independent quantities are the  $\alpha$ -widths  $\gamma_\alpha^2$  as these are the quantities best determined in a nuclear reaction. Fortunately, these are precisely the factors needed in astrophysical calculations.

#### 4.2. ALPHA WIDTHS

The reduced  $\alpha$ -width  $\gamma_\alpha^2$  is defined here as <sup>22-24)</sup>

$$\gamma_\alpha^2(s) = \frac{\hbar^2 s}{2\mu_\alpha} |R_L(s)|^2, \quad (2)$$

where the quantity "s" is the channel radius,  $\mu_\alpha$  is the reduced mass and  $R_L(s)$  is the radial part of the  $\alpha + {}^{12}\text{C}$  cluster wave function at  $r = s$ . The  $\alpha$ -width,  $\Gamma_\alpha$ , for an  $\alpha$ -unbound level is then given by

$$\Gamma_\alpha = 2\gamma_\alpha^2(s)P_L(Q_\alpha, s), \quad (3)$$

where  $P_L(Q_\alpha, s)$  is the  $\alpha$ -penetrability for an  $\alpha$ -decay energy,  $Q_\alpha$ .

The quantity  $\Gamma_\alpha$  is the formal R-matrix  $\alpha$ -width and not necessarily equal to the observed line width,  $\Gamma_{\text{c.m.}}$ , for  $\alpha$ -unbound levels. The two widths are often comparable in value and become identical in certain one-level approximations <sup>22)</sup>. Thus  $\Gamma_\alpha$  and  $\Gamma_{\text{c.m.}}$  are often used interchangeably in the literature <sup>14)</sup>. We also often will assume  $\Gamma_\alpha = \Gamma_{\text{c.m.}}$  (table 1), although this may affect comparisons with  $\Gamma_\alpha$  deduced from R-matrix analyses.

The  $\alpha$ -spectroscopic factor,  $S_\alpha$ , is related to  $R_L(r)$  in (2) by

$$R_L(r) = \sqrt{S_\alpha} R_L^{\text{PW}}(r), \quad (4)$$

where  $R_L^{\text{DW}}(r)$  is the model wave function for  $\alpha + {}^{12}\text{C}$  utilized in the distorted-wave calculations. Thus

$$\gamma_\alpha^2(s) = S_\alpha \frac{\hbar^2 s}{2\mu_\alpha} |R_L^{\text{DW}}(s)|^2. \quad (5)$$

It is customary to scale  $\gamma_\alpha^2$  (or  $\Gamma_\alpha$ ) by the corresponding Wigner limits <sup>24)</sup>

$$\gamma_{\text{W}}^2(s) = 3\hbar^2/2\mu_\alpha s^2, \quad (6)$$

$$\Gamma_{\text{W}}(s) = 2\gamma_{\text{W}}^2(s)P_L(Q_\alpha, s),$$

and define the dimensionless  $\alpha$ -reduced width by

$$\theta_\alpha^2(s) = \gamma_\alpha^2(s)/\gamma_{\text{W}}^2(s) = \Gamma_\alpha/\Gamma_{\text{W}}. \quad (7)$$

Transfer reactions involving strongly absorbed projectiles such as  ${}^7\text{Li}$  are sensitive to  $R_L(r)$  primarily at the nuclear surface. One therefore should choose a channel radius,  $s$ , appropriate to the particular reaction as  $\gamma_\alpha^2$  will then not depend on the precise form of the model wave function <sup>23)</sup>. This is important for unbound levels such as the 9.6 MeV  $1^-$  state as then  $\gamma_\alpha^2$  is not greatly affected by extrapolation into the continuum. We choose  $s = 5.4$  fm as this satisfies the above criterion and also corresponds to the channel radius commonly used in analyses of other experiments, permitting a direct comparison of  $\gamma_\alpha^2$ . Note that  $\theta_\alpha^2 = 1$  does not necessarily imply  $S_\alpha = 1$  as  $\gamma_{\text{W}}^2(s)$  corresponds to a particularly simple choice for  $R_L(s)$ , whereas Coulomb and other effects should be included <sup>24)</sup>. Thus  $\theta_\alpha^2 \approx 1$  and  $S_\alpha < 1$  may be compatible for a particular choice of  $R_L(s)$ . Conversely,  $S_\alpha < 1$  does not always imply  $\theta_\alpha^2 < 1$  as is often assumed in extracting  $\theta_\alpha^2$  values for levels in  ${}^{16}\text{O}$ , particularly the 7.12 MeV  $1^-$  state.

The values of  $\gamma_\alpha^2(s)$ ,  $\theta_\alpha^2(s)$  and  $\Gamma_\alpha$  deduced from our analysis are listed in table 2. Although these in principle are again "absolute" values, only the relative values or ratios are determined with any reliability. It is reassuring, however, that using fixed, "realistic"  ${}^7\text{Li}$  wave functions, optical model and bound-state parameters yields absolute cross sections comparable to the experimental values for reasonable values of  $S_\alpha$ . This gives additional credibility to our assumptions concerning the reaction mechanism.

The relative values of  $\gamma_\alpha^2$  and  $\theta_\alpha^2$  for members of rotational bands are similar, as expected, except for the 6 MeV  $0^+$  bandhead which has smaller values. The 7.1 MeV level indicates  $S_\alpha \approx 0.3$ , when compared relative to the  $4^+$  (10.35 MeV) state for our preferred optical model set. This is compatible with the measurements of ref. <sup>10)</sup> at  $E({}^7\text{Li}) = 38$  MeV. We note that  $S_\alpha \approx \theta_\alpha^2 \approx 0.6$  for the 9.6 MeV state relative to the  $4^+$  level, however. Our results for  $\theta_\alpha^2(5.4 \text{ fm})$  are in only fair agreement with the  ${}^{12}\text{C}({}^7\text{Li}, t){}^{16}\text{O}$  measurements of Pühlhofer *et al.* <sup>8)</sup> at  $E({}^7\text{Li}) \approx 20$  MeV but our DWBA analyses differ substantially, in that we include the recoil  $l$ -transfers explicitly. Whereas we obtain  $\theta_\alpha^2(7.1 \text{ MeV})/\theta_\alpha^2(4^+, 10.3 \text{ MeV}) = 0.28$ , they obtain  $\theta_\alpha^2(7.1 \text{ MeV})/\theta_\alpha^2(4^+) = 0.08$  to 0.25, depending on the value used for  $\theta_\alpha^2(4^+)$ ,

Dimensionless reduced  $\alpha$ -widths,  $\theta_\alpha^2$ , for unbound states in  $^{16}\text{O}$  have been deduced from experimental and calculated  $\alpha$ -widths by Suzuki<sup>13</sup>). His analysis ( $s = 5.4$  fm) indicates  $\theta_\alpha^2(9.6 \text{ MeV}) = 0.70$  for  $\Gamma_\alpha = 510$  keV and  $\theta_\alpha^2(4^+) = 0.34$  for  $\Gamma_\alpha = 27$  keV. Our values for  $\Gamma_{\text{c.m.}}$  (table 1) assuming  $\Gamma_\alpha = \Gamma_{\text{c.m.}}$  then imply  $\theta_\alpha^2(9.6 \text{ MeV}) = 0.054 \pm 0.07$  and  $\theta_\alpha^2(4^+) = 0.44 \pm 0.06$ . Combining these with out ratios for  $\theta_\alpha^2(7.1)/\theta_\alpha^2(9.6)$  and  $\theta_\alpha^2(7.1)/\theta_\alpha^2(4^+)$  from table 2 yields  $\theta_\alpha^2(7.1) = 0.19 \pm 0.07$  and  $\theta_\alpha^2(7.1) = 0.12 \pm 0.02$ , respectively. Including reasonable  $R$ -matrix level-shift parameters for the 9.6 MeV level indicates  $\Gamma_\alpha > \Gamma_{\text{c.m.}}$  by perhaps 20% at  $s = 5.4$  fm, however, which would increase  $\theta_\alpha^2(9.6 \text{ MeV})$  and hence  $\theta_\alpha^2(7.1 \text{ MeV})$  by a comparable amount. Additional uncertainties of typically  $\pm 30\%$  are introduced due to relative variations in  $\theta_\alpha^2$  with optical model parameters. Including these in a statistical fashion with the previous values for  $\theta_\alpha^2$ , gives

$$0.09 < \theta_\alpha^2(7.1 \text{ MeV}) < 0.33,$$

with a weighted mean of

$$\theta_\alpha^2(7.1) = 0.14 \pm 0.04. \quad (8)$$

We believe the above results to be the most self-consistent model-independent ones that can be extracted from the present transfer data. These results are in good agreement with limits determined from a recent analysis of  $^{12}\text{C}(^6\text{Li}, d)$  at  $E = 42$  MeV, which indicates  $0.1 < \theta_\alpha^2(7.1 \text{ MeV}) < 0.4$ . The values of  $\theta_\alpha^2(7.1 \text{ MeV})$  deduced from ( $^7\text{Li}, t$ ) and ( $^6\text{Li}, d$ ) experiments appear to exclude values of  $\theta_\alpha^2(7.1 \text{ MeV}) \ll 0.10$ , which excludes the lower limits of several other determinations<sup>3, 25-30</sup>) of  $\theta_\alpha^2(7.1)$ :  $^{12}\text{C} + \alpha$  scattering ( $0.06 < \theta_\alpha^2 < 0.24$ ),  $^{16}\text{N}$  decay ( $0.01 < \theta_\alpha^2 < 0.11$ ), C/O abundances ( $0.01 < \theta_\alpha^2 \ll 0.08$ ) and early shell-model calculations ( $0.04 < \theta_\alpha^2 < 0.12$ ). The apparent agreement with recent hybrid  $R$ -matrix calculations, which indicate  $0.08 < \theta_\alpha^2 < 0.32$  is not valid as  $\theta_\alpha^2$  is defined in a different manner<sup>28, 31</sup>). This is discussed in the following section. We are in agreement with recent cluster-model calculations ( $\theta_\alpha^2 \approx 0.15$ ), although our value for  $\theta_\alpha^2(9.6 \text{ MeV})$  is slightly smaller<sup>13</sup>).

#### 4.3. THE RATIO $\theta_\alpha^2(7.1 \text{ MeV})/\theta_\alpha^2(9.6 \text{ MeV})$

It is convenient in comparing the various determinations of  $\theta_\alpha^2$  to consider the ratio,  $R$ , where

$$\begin{aligned} R &\equiv \gamma_\alpha^2(7.1 \text{ MeV})/\gamma_\alpha^2(9.6 \text{ MeV}) \\ &= \theta_\alpha^2(7.1 \text{ MeV})/\theta_\alpha^2(9.6 \text{ MeV}), \end{aligned} \quad (9)$$

as this quantity should be less model dependent than  $\gamma_\alpha^2$  or  $\theta_\alpha^2$  alone.

The ratio,  $R$ , of reduced  $\alpha$ -widths for the  $1^-$  states of astrophysical interests determined in this experiment has the value  $R = 0.41$  for our preferred  $^7\text{Li}$  optical model

set;  $R = 0.46$  [ ${}^7\text{Li}$  set of ref. <sup>20</sup>];  $R = 0.23$  [ ${}^7\text{Li}$  set IV of ref. <sup>19</sup>];  $R = 0.15$  [ ${}^7\text{Li}$  set of ref. <sup>10</sup>]; and  $R = 0.28$  [ ${}^7\text{Li}$  set of ref. <sup>10</sup>; 3 fm radial cut off]. Calculations utilizing other  $\alpha + {}^{12}\text{C}$  model wave functions (table 2) give  $R = 0.29, 0.39$  and  $0.55$ . Alternatively, one may choose to ignore our determination of  $\theta_\alpha^2(9.6 \text{ MeV})$  and use only our value for  $\theta_\alpha^2(7.1 \text{ MeV})/\theta_\alpha^2(4^+)$  with  $\theta_\alpha^2(9.6 \text{ MeV})$  taken to be  $0.85$ , a generally accepted value <sup>2,3</sup>). This yields  $R = 0.33$ , or  $R = 0.10$  to  $0.40$  depending on the  ${}^7\text{Li}$  optical model parameters used.

The preceding values for  $R$  are to be compared with the cross section ratios  $\sigma_{\text{exp}}(7.1)/\sigma_{\text{exp}}(9.6) = 0.53$  and  $\sigma_{\text{dir}}(7.1)/\sigma_{\text{dir}}(9.6) = 0.36$ . As expected for this type of reaction <sup>23</sup>) the ratio of  $\sigma_{\text{dir}}$  corresponds closely to our inferred ratio  $R$ . The quantity  $R$  depends on the magnitude and coherence of the non-direct component,  $\sigma_{\text{HF}}$ . Our values for  $\sigma_{\text{HF}}$  are likely upper limits as we over-estimate the observed cross sections at large angles (fig. 5). An estimate of the uncertainty in  $\sigma_{\text{HF}}$  suggests  $R = 0.45$  as a probable upper limit. The mean value of all the above determinations of  $R$  and the rms deviation is

$$R = 0.35 \pm 0.13.$$

Our analysis based on the present ( ${}^7\text{Li}, t$ ) data and the proviso  $\sigma_{\text{dir}} \approx \sigma_{\text{exp}} - \sigma_{\text{HF}}$  would exclude  $R < 0.10$ .

We compare, in fig. 7, the ratio  $R$  determined in the present experiment with other, inferred experimental and theoretical values. The upper limits for the  $\gamma_\alpha^2$  values for the SU(3) and OCM theories have been calculated from the theoretical  $S_\alpha$  values and our radial wave function for  $R_L(r)$  via eq. (5). The lower limits correspond to the

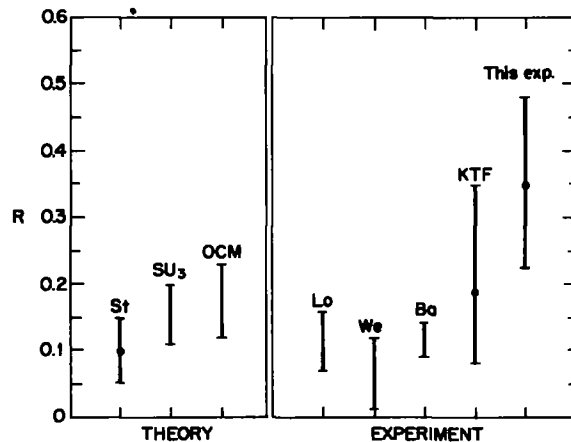


Fig. 7. A comparison of calculated and experimental values for the ratio,  $R$ , defined as  $\theta_\alpha^2(7.1 \text{ MeV})/\theta_\alpha^2(9.6 \text{ MeV})$ , St: ref. <sup>25</sup>); SU(3): ref. <sup>12</sup>); OCM: ref. <sup>13</sup>); Lo:  ${}^6\text{Li}({}^{12}\text{C}, d){}^{16}\text{O}$ , ref. <sup>5</sup>); We:  ${}^{16}\text{N}$  decay, ref. <sup>26</sup>); Ba:  ${}^{12}\text{C}(\alpha, \alpha)$  and  ${}^{16}\text{N}$  decay, ref. <sup>27</sup>); KTF:  ${}^{12}\text{C}(\alpha, \alpha)$  and  ${}^{12}\text{C}(\alpha, \gamma)$ , ref. <sup>28</sup>) (see also ref. <sup>29</sup>). A recent  ${}^{12}\text{C}({}^6\text{Li}, d){}^{16}\text{O}$  experiment yields  $R = 0.6^{+1.7}_{-0.3}$  (ref. <sup>11</sup>)). See text regarding definitions of  $\theta_\alpha^2$  however.



ratio of  $S_\alpha$  values alone. The other calculation is that due to Stephenson<sup>25</sup>). He assumes a 3p-3h configuration ( $\lambda\mu = 63$ ) as the major component for the 9.6 MeV  $1^-$  level whereas the other calculations use 4p-4h ( $\lambda\mu = 94$ ), which should be more realistic. Surprisingly, perhaps, Stephenson's value is less than that deduced from the more recent calculations. The experimental values shown come from many sources:  $^6\text{Li}(^{12}\text{C}, d)^{16}\text{O}$  [ref. 5)]; decay of  $^{16}\text{N}$  [ref. 26)]; analyses of  $^{12}\text{C}(\alpha, \alpha)^{12}\text{C}$  and  $^{12}\text{C}(\alpha, \gamma)^{16}\text{O}$  [refs. 27, 28)], and our results for ( $^7\text{Li}, t$ ). A recent analysis<sup>11</sup>) of  $^{12}\text{C}(^6\text{Li}, d)^{16}\text{O}$  yields  $R = 0.6_{-0.3}^{+1.7}$  (not shown). Although other  $\alpha$ -transfer data exist, the ratio  $R$  has not been explicitly extracted although  $S_\alpha(7.1)$  or  $\theta_\alpha^2(7.1)$  values are quoted<sup>6-30</sup>). An examination of the published data suggests  $R > 0.10$ , however, which is consistent with the present measurement. Recall, however, that our analysis also indicates  $\Gamma_{\text{c.m.}}(9.6 \text{ MeV}) = 390 \pm 60 \text{ keV}$  and  $\theta_\alpha^2(9.6 \text{ MeV}) \approx 0.6$  which are smaller than the "accepted" values ( $510 \pm 60 \text{ keV}$  and 0.85, respectively).

Our value for  $R$  appears to be substantially larger (factor of two or more) compared with other determinations. There is overlap with the upper limits of the most recent analyses<sup>28-30</sup>) of  $^{12}\text{C}(\alpha, \gamma)^{16}\text{O}$ , but one must use caution in making such comparisons (see below).

The larger  $R$ -value determined in the present experiment is not necessarily due to a larger  $\theta_\alpha^2(7.1 \text{ MeV})$  but is mainly due to a smaller  $\theta_\alpha^2(9.6 \text{ MeV})$ . Similarly our values for  $\theta_\alpha^2(10.3 \text{ MeV})$  and  $\theta_\alpha^2(6.9 \text{ MeV})$  tend to be smaller than other determinations so that  $\theta_\alpha^2(7.1)$  is still significant compared to  $\theta_\alpha^2$  for " $\alpha$ -cluster" levels in  $^{16}\text{O}$ . We note that  $\theta_\alpha^2$  (or  $S_\alpha$ ) is not necessarily expected to be equal to unity even for  $\alpha$ -cluster states owing to antisymmetrization. Thus the simple SU(3) limits indicate<sup>12</sup>)  $\theta_\alpha^2 < 0.3$  while OCM calculations<sup>13</sup>) give  $\theta_\alpha^2 < 0.6$ , which appears to be consistent with data for many levels in  $^{16}\text{O}$ .

## 5. Stellar helium burning rates

The stellar temperatures of interest in helium burning correspond to an  $\alpha + ^{12}\text{C}$  energy in the c.m. system of about 300 keV [refs. 1-3)]. At present a large extrapolation of existing  $^{12}\text{C}(\alpha, \gamma)^{16}\text{O}$  data<sup>1</sup>) is thus required. This is normally done by fitting data for  $^{12}\text{C} + \alpha$  resonances,  $^{16}\text{N}$  decay as well as  $^{12}\text{C}(\alpha, \gamma)^{16}\text{O}$  with  $\theta_\alpha^2(7.1 \text{ MeV})$  and  $\theta_\alpha^2(9.6 \text{ MeV})$  adjusted to obtain a "best" fit. The reaction rate for  $^{12}\text{C}(\alpha, \gamma)$  at  $E_{\text{c.m.}} = 300 \text{ keV}$ , denoted  $S(300 \text{ keV})$  with units in  $\text{MeV} \cdot \text{b}$ , appears to depend mostly on  $\theta_\alpha^2(7.1 \text{ MeV})$  [refs. 2, 27)]. Although the exact relation between  $S(300 \text{ keV})$  and  $\theta_\alpha^2(7.1 \text{ MeV})$  is influenced by the interference with other  $J^\pi = 1^-$  levels, a simple one-level approximation suggests  $S(300 \text{ keV}) \propto \theta_\alpha^2(7.1 \text{ MeV})$ . Unfortunately, the exact scaling between  $S(300 \text{ keV})$  and  $\theta_\alpha^2(7.1 \text{ MeV})$  varies considerably for the various published  $R$ -matrix analyses<sup>27-30</sup>). The differences appear to be related to the particular choice of certain  $R$ -matrix boundary conditions even though the same channel radii are utilized ( $s = 5.4 \text{ fm}$ ). Thus the results from ref. 2) indicate  $S(300 \text{ keV}) = 1.42 \theta_\alpha^2 \text{ MeV} \cdot \text{b}$ ; ref. 27),  $S(300 \text{ keV}) = (1.7 \pm 0.4) \theta_\alpha^2 \text{ MeV} \cdot \text{b}$ ; ref. 28),  $S(300 \text{ keV}) =$

$0.44 \theta_\alpha^2 \text{ MeV} \cdot \text{b}$ ; ref. <sup>30</sup>),  $S(300 \text{ keV}) = 2.5 \theta_\alpha^2 \text{ MeV} \cdot \text{b}$ . The conventional  $R$ -matrix formulations [refs. <sup>2, 27, 30</sup>] suggest  $S(300 \text{ keV}) = (2.0 \pm 0.6) \theta_\alpha^2(7.1 \text{ MeV}) \text{ MeV} \cdot \text{b}$ , while the hybrid  $R$ -matrix calculations <sup>28</sup>) apparently have quite different implications.

It appears that the determination of  $\theta_\alpha^2(7.1 \text{ MeV})$  using an  $\alpha$ -transfer reaction such as ( ${}^7\text{Li}, t$ ) corresponds to the simple one-level definition of  $\theta_\alpha^2$  which excludes energy shifts, etc. <sup>22</sup>). It is known, however, that the 9.6 MeV level interferes constructively <sup>1</sup>) at  $E_{c.m.} \approx 300 \text{ keV}$  which increases  $S(300 \text{ keV})$  by about 30%. This accounts for the differences between the results of refs. <sup>2, 27</sup>). The results of a conventional  $R$ -matrix analysis <sup>27</sup>) with our value for  $\theta_\alpha^2(7.1 \text{ MeV})$  yields

$$0.15 \text{ MeV} \cdot \text{b} \lesssim S(300 \text{ keV}) \lesssim 0.36 \text{ MeV} \cdot \text{b},$$

with a mean value

$$S(300 \text{ keV}) = 0.24 \pm 0.09 \text{ MeV} \cdot \text{b}. \quad (12)$$

In contrast, extrapolating the hybrid  $R$ -matrix analysis <sup>28</sup>) in terms of  $\theta_\alpha^2$  suggests  $0.04 \text{ MeV} \cdot \text{b} < S(300 \text{ keV}) < 0.15 \text{ MeV} \cdot \text{b}$  but such a procedure is not valid because of the different  $\theta_\alpha^2$  employed <sup>27, 31</sup>). Scaling  $\theta_\alpha^2$  for this <sup>27, 31</sup>) implies  $\theta_\alpha^2 = 0.03$  for  $S(300 \text{ keV}) = 0.08$  or  $S(300 \text{ keV}) = 2.6 \theta_\alpha^2 \text{ MeV} \cdot \text{b}$ , which more closely corresponds to other analyses. Using the latter then gives  $S(300 \text{ keV}) = 0.36 \pm 0.10 \text{ MeV} \cdot \text{b}$  for our value of  $\theta_\alpha^2(7.1 \text{ MeV})$ . Another procedure is to use a value of  $\theta_\alpha^2(7.1 \text{ MeV})$  extracted from the ratio  $R$  (eq. (9)) and use  $\theta_\alpha^2(9.6 \text{ MeV})$  determined in the hybrid  $R$ -matrix analysis. This removes some of the scaling in  $\theta_\alpha^2$  arising from different boundary conditions and  $\alpha$ - ${}^{12}\text{C}$  model wave functions <sup>22, 23, 27</sup>). Such a procedure gives  $S(300 \text{ keV}) = 0.13 \pm 0.04 \text{ MeV} \cdot \text{b}$ .

Considering the above results, the present  $\alpha$ -transfer, data with  $\theta_\alpha^2(7.1 \text{ MeV})$  interpreted in a manner we believe to be most consistent with the reaction analysis (sect. 4) indicates

$$0.09 \text{ MeV} \cdot \text{b} < S(300 \text{ keV}) < 0.46 \text{ MeV} \cdot \text{b}. \quad (13)$$

This result is to be compared with  $S(300 \text{ keV}) = 0.14_{-0.12}^{+0.14} \text{ MeV} \cdot \text{b}$  [ref. <sup>1</sup>)],  $S(300 \text{ keV}) \approx 0.25 \text{ MeV} \cdot \text{b}$  [ref. <sup>27</sup>)],  $S(300 \text{ keV}) = 0.08_{-0.04}^{+0.05} \text{ MeV} \cdot \text{b}$  [ref. <sup>28</sup>)] and  $S(300 \text{ keV}) = 0.08_{-0.07}^{+0.14} \text{ MeV} \cdot \text{b}$  [ref. <sup>29</sup>)]. The lower limits on  $S(300 \text{ keV})$  given by (13) thus overlap with the upper limits of several other analyses but would exclude  $S(300 \text{ keV}) \ll 0.1 \text{ MeV} \cdot \text{b}$ .

A large helium burning rate would rapidly deplete carbon during the helium burning phase of stellar evolution. An estimate of the final mass fraction of carbon,  $X_C$ , has been derived by Arnett <sup>3</sup>) and others <sup>4</sup>) in terms of  $\theta_\alpha^2(7.12 \text{ MeV})$  based on the relation between  $S(300 \text{ keV})$  and  $\theta_\alpha^2(7.12 \text{ MeV})$  appropriate for a one-level  $R$ -matrix <sup>2</sup>). Including constructive interference from other levels increases  $S(300 \text{ keV})$  for a given  $\theta_\alpha^2(7.12 \text{ MeV})$ , as noted previously. Thus our  $\theta_\alpha^2(7.12 \text{ MeV}) = 0.14 \pm 0.04$  effectively corresponds to a large " $\theta_\alpha^2$ " in Arnett's expressions, *viz.* " $\theta_\alpha^2$ " =  $0.17 \pm 0.06$ .

Inserting the latter in Arnett's expression for  $X_C$  implies <sup>3,4)</sup>  $0.07 < X_C < 0.27$  for  $M_a/M_\odot = 8$  and  $X_C < 0.51$  for  $M_a/M_\odot = 1$ , where  $M_a/M_\odot$  is the helium core mass in solar mass units. These values for  $X_C$  are smaller than those deduced from the known  $^{12}\text{C}/^{16}\text{O}$  abundances in the solar system utilizing existing models of stellar evolution <sup>3,4)</sup>. Smaller values for  $X_C$  would imply an oxygen enrichment ( $X_O \approx 1 - X_C$ ) and would lead to increased synthesis of  $^{20}\text{Ne}$  and heavier elements <sup>2,3)</sup> which would affect the scenario of supernovae and neutron star formation.

The above conclusions, of course, depend on the validity of the existing models for stellar evolution and the exact correlation between the  $^{12}\text{C}(\alpha, \gamma)$  reaction rate,  $\theta_\alpha^2(7.1 \text{ MeV})$  and the ratio  $R \equiv \theta_\alpha^2(7.1 \text{ MeV})/\theta_\alpha^2(9.6 \text{ MeV})$ . Better clarification of this relation would be clearly desirable. In any event it appears that data from  $\alpha$ -transfer reactions cannot be used to justify  $\theta_\alpha^2(7.1 \text{ MeV}) \ll 0.1$  or  $R < 0.1$  and the implications for  $\theta_\alpha^2(7.1 \text{ MeV})$  and  $R > 0.1$  should be considered in any nucleosynthesis calculations.

The authors thank Profs. K. T. Hecht, J. Janecke, P. Parker, C. Barnes, T. Tombrello, S. Austin, F. Barker and W. Fowler for useful comments and discussions. One of us (F.D.B.) also thanks the staffs of LASL and Kellogg Radiation Laboratory (Cal. Inst. Tech.) for their hospitality and financial assistance during the course of this work.

### References

- 1) P. Dyer and C. A. Barnes, Nucl. Phys. **A233** (1974) 495
- 2) W. A. Fowler, G. R. Caughlan and B. A. Zimmerman, Ann. Rev. Astron. and Astrophys. **5** (1967) 525; **13** (1975) 69
- 3) W. D. Arnett, Astrophys. J. **176** (1972) 681; **170** (1971) L43
- 4) W. Deinzer and E. E. Salpeter, Astrophys. J. **140** (1964) 499
- 5) H. M. Loebenstein, D. W. Mingay, H. Winkler and C. S. Zaidins, Nucl. Phys. **A91** (1967) 481
- 6) K. Bethge, Ann. Rev. Nucl. Sci. **20** (1970) 255
- 7) V. Z. Gol'dberg *et al.*, Izv. Akad. Nauk (ser. fiz.) **33** (1969) 566
- 8) F. Pühlhofer, H. G. Ritter, R. Bock, G. Brommundt, H. Schmidt and K. Bethge, Nucl. Phys. **A147** (1970) 528
- 9) A. A. Ogloblin, Fiz. Elem. Chast. Atom. Yad. **3** (1972) 936 [English translation: Sov. J. Part. and Nuclei **3** (1973) 467]
- 10) M. E. Cobern, D. J. Pisano and P. D. Parker, Phys. Rev. **C14** (1976) 491
- 11) F. D. Becchetti, J. Janecke and C. E. Thorn, **A305** (1978) 313
- 12) M. Ichimura, A. Arima, E. C. Halbert and T. Terasawa, Nucl. Phys. **A204** (1973) 225; K. T. Hecht, private communication; D. Strottman and D. J. Millener, Proc. Int. Conf. on nuclear reactions, vol. 1, ed. J. de Boer and H. J. Mang (North-Holland, Amsterdam, 1973) p. 107
- 13) Y. Suzuki, Prog. Theor. Phys. **55** (1976) 1751; **56** (1976) 111
- 14) F. Ajzenberg-Selove, Nucl. Phys. **A281** (1977) 1
- 15) E. R. Flynn, S. Orbesen, J. D. Sherman, J. W. Sunier and R. Woods, Nucl. Instr. **128** (1975) 35
- 16) R. M. DeVries, Phys. Rev. **C8** (1973) 951; Program LOLA, unpublished
- 17) K. I. Kubo and M. Hirata, Nucl. Phys. **A187** (1972) 186
- 18) J. D. Garrett and O. Hansen, Nucl. Phys. **A212** (1973) 600
- 19) P. Schumacher, N. Veta, H. H. Duhm, K. I. Kubo and W. J. Klages, Nucl. Phys. **A212** (1973) 573
- 20) J. E. Poling, E. Norbeck and R. R. Carlson, Phys. Rev. **C13** (1976) 648
- 21) R. Huby and J. R. Mince, Rev. Mod. Phys. **37** (1965) 406

- 22) A. M. Lane and R. G. Thomas, *Rev. Mod. Phys.* **30** (1958) 328
- 23) F. L. Milder, J. Jänecke and F. D. Becchetti, *Nucl. Phys.* **A276** (1977) 72
- 24) A. Bohr and B. R. Mottelson, *Nuclear structure*, vol. 1 (Benjamin, NY, 1970) p. 441
- 25) G. J. Stephenson, Jr., *Astrophys. J.* **3** (1966) 950
- 26) C. Wertz, *Phys. Rev.* **C4** (1971) 1591
- 27) F. C. Barker, *Austral. J. Phys.* **24** (1971) 777, and private communication (1978)
- 28) S. E. Koonin, T. A. Tombrello and G. Fox, *Nucl. Phys.* **A220** (1974) 221
- 29) J. Humblet, P. Dyer and B. A. Zimmerman, *Nucl. Phys.* **A271** (1976) 210
- 30) D. C. Weisser, J. F. Morgan and D. R. Thompson, *Nucl. Phys.* **A235** (1974) 460
- 31) T. Tombrello, private communication (1978)